QUATERNARY OSTRACODE PALEOECOLOGY AND ITS LINK TO CLIMATE CHANGE IN THE BONNEVILLE BASIN: A DETAILED STUDY OF THE GLAD800 CORE GSL00-4, GREAT SALT LAKE, UTAH

By

Deborah P. Balch, Andrew Cohen, J.Warren Beck and R. Lawrence Edwards

A Prepublication Manuscript Submitted to the Faculty of the

DEPARTMENT OF GEOSCIENCES

In Partial Fulfillment of the Requirements
For the Degree of

MASTER OF SCIENCE

In the Graduate College
THE UNIVERSITY OF ARIZONA
2003

STATEMENT BY THE AUTHOR

This manuscript, prepared for publication in the *(insert the name of journal, series, etc.)*, has been submitted in partial fulfillment of requirements for the Master of Science degree at The University of Arizona and is deposited in the Antevs Reading Room to be made available to borrowers, as are copies of regular theses and dissertations.

Brief quotations from this manuscript are allowable without special permission, provided that accurate acknowledgement of the source is made. Requests for permission for extended quotation from or reproduction of this manuscript in whole or in part may be granted by the Department of Geosciences when the proposed use of the material is in the interests of scholarship. In all other instances, however, permission must be obtained from the author.

(author's signature) 8-11-2003 *(date)*

APPROVAL BY RESEARCH COMMITTEE

As members of the Research Committee, we recommend that this prepublication manuscript be accepted as fulfilling the research requirement for the degree of Master of Science.

Andrew Cohen — 8/14/03
Major Advisor *(type name)* *(signature)* *(date)*

Karen W. Flessa — 8/11/03
(type name) (signature) (date)

Owen Davis — 8/15/03
(type name) (signature) (date)

ABSTRACT

We report the results of a detailed paleoecological study of the Bonneville Basin covering the last ~240,000 years. Our study used fossil ostracodes and a sedimentological record obtained from the August 2000 GLAD800 drilling operation at the Great Salt Lake. We analyzed 125 samples, taken at ~1 meter intervals from core GSL00-4, for ostracodes and other paleoecologic and sedimentological indicators of environmental change. Multivariate analyses applied to the ostracode data indicate an alternation between three major environments at the core site over the cored interval. The environments fluctuated most often between shallow saline, open-water lake conditions (when the lake was high enough to inundate the core site) and salt or freshwater, spring-fed marsh (when the water level was at or lower than the core site). But occasionally, the core site was submerged by deep fresh water. Immediately following deep lake phases, crashes in lake level from rapid desiccation resulted in the deposition of thick evaporite units. These environmental changes are consistent with shoreline studies of regional lake level fluctuations, but provide considerable new detail on both the timing and environmental conditions associated with the various lake phases. Our age model (using dates obtained from ^{14}C, U-series, tephra and biostratigraphic chronologies) allowed us to associate the core's record of regional paleohydrology to the marine oxygen isotope stages record of global climate change. The core contains high resolution, continuous records for the last three glacial/interglacial sequences. In each case we found that fresh open-water conditions (i.e. lake highstands) correspond with maximum glacial advances, except for the smaller, less intense OIS 4 glaciation, when the lake remained saline. Salt and freshwater marshes were dominant environments for most of the interglacials. However, throughout most of the Quaternary, this basin has contained a shallow, saline open-water lake.

INTRODUCTION

In the late 1990's, the International Continental Drilling Program (ICDP) provided the funds for DOSECC (the US nonprofit research consortium for continental scientific drilling) to develop a dedicated lake drilling system, designated the GLAD800 system. The intent of this grant was to jump start scientific drilling in lakes around the world with an inexpensive and modular system that would be easily transported between sites, and would be broadly accessible to the scientific community. This system, including a barge platform, drill rig and coring tool kit, was first tested with NSF support at the Great Salt Lake and Bear Lake in August 2000. The mandate from NSF was that all engineering tests of the GLAD-800 system be coupled to significant scientific questions, so that the testing would also yield scientific benefits. The long history of scientific (and specifically paleoclimate) research on the Great Salt Lake, dating back to the 19th Century (Gilbert, 1890) coupled with DOSECC's location in Salt Lake City, made the Great Salt Lake and Bear Lake natural targets for this testing.

The drilling campaign collected four long cores from the Great Salt Lake and obtained a total of 371m of sediment with 96% recovery. One core in particular, GSL00-4, reached 121 meters below lake floor (mblf) and provides the longest continuous record of the lake's history ever collected from a drilling operation. Drilling for GSL00-4 took place in the hanging wall of the Carrington Fault, which is located along the southeast margin of the lake's northern basin (Fig.1). The primary objective for drilling at this site was to obtain a detailed basinal history extending back to Oxygen Isotope Stage (OIS) 6 and to use its paleontological and sedimentological contents to address questions related to paleoclimate.

A preliminary study of the core, based on core catcher samples taken every 3 meters (ca. 6000 year resolution), suggested that GSL00-4 contains a high-resolution paleoecological record extending back ~250,000 yr BP based on tephra correlation and preliminary U-series dating (Dean *et al.* 2002). Paleoecological analyses of its ostracode assemblages, in particular, have shown that the lake levels have fluctuated over time giving rise to both marsh conditions and saline, open water conditions at the core site (Kowalewska and Cohen, 1998; Dean *et. al* 2002). Up to this point, we did not have detailed knowledge about these environmental fluctuations because the previous studies were at too low of a resolution. The goal of this current study was to explain these patterns in greater detail by accomplishing the following: (i) increase sampling frequency to improve resolution; (ii) resolve the chronological sequence of paleoecological and paleolimnological change through the acquisition of a reliable age model; and (iii) determine if these changes are correlated with changes in regional or global climate change, particularly at the glacial/interglacial time scale.

Previous Research

The Bonneville Basin, located in the northeastern Great Basin, has been a major focus of North American Quaternary research for more than a century. G.K. Gilbert (1890) was the first to recognize that the basin contains excellent stratigraphic records of past environmental change. By studying its lacustrine deposits, he reconstructed the history of Lake Bonneville, emphasizing its dramatic transgressions and regressions during the late Pleistocene. In 1948, Ernst Antevs proposed a correlation between the maximum height of Lake Bonneville and the maximum extent of local mountain glaciers (see Oviatt, 2002).

Research in the late 20th century has provided evidence that as many as four deep lake cycles have occurred in the Bonneville Basin over the past 500,000 years. Modeling results suggest that at least the most recent of these lake level fluctuations (the "Lake Bonneville" phase) may have been linked to the southward migration of the jet stream during Northern Hemisphere glacial advance (Thompson *et al.* 1993; Kutzbach *et al.* 1994; COHMAP,1988). A southward migration of the jet stream from its current position could be expected to bring more precipitation to the eastern Great Basin and, therefore, lakes in the eastern Great Basin become deeper during the glacial advance. Because of its abundant evidence from shoreline terrace deposits, the Late Pleistocene Lake Bonneville phase has been the most intensively studied of all the deep lake cycles. High stands in this most recent deep lake cycle are clearly correlated with the most recent glacial advance (i.e. Spencer *et al.* 1984; Currey and Oviatt, 1985; Oviatt *et al.* 1992; Oviatt, 1997; Oviatt *et al.* 1999). However, earlier deep lake cycles also appear to be associated in time with the global oxygen isotope record. The deep lake cycle known as Cutler Dam preceded Lake Bonneville, and has been correlated with the OIS 4/OIS 3 transition (Oviatt *et al.* 1987; Kaufman *et al.* 2001). Two older deep lake cycles, the Little Valley cycle, which has been associated with glacial stage OIS 6 (Scott *et al.* 1983; Oviatt *et al.* 1999) and the Pokes Point cycle, associated with OIS 12 (Oviatt *et al.* 1999), are also known from outcrops but remain poorly understood.

Today, all that remains of Lake Bonneville is a patch of briny water, otherwise known as the Great Salt Lake. Buried deep beneath this lake is a well-preserved stratigraphic record the Bonneville Basin's climate-driven past. Wells drilled by Amoco Production Company in the late 1970's provided researchers with evidence that the sediments beneath the Great Salt Lake contain one of the most continuous Neogene records of North American climate and

environmental change (Davis, 1998; Davis and Moutoux, 1998; Kowalewska and Cohen, 1998). Obtaining a long, continuous core from this basin has the potential to give one of the best and most complete paleoclimate records to date and this is one of the primary reasons DOSECC chose the Great Salt Lake as its first test of the GLAD 800 Drilling system.

METHODS

To accomplish our goals, we have assembled a ~2,000 yr resolution paleoenvironmental record using GSL00-4's lithology and fossil invertebrates as indicators of environmental and ecosystem response to climate change. We have chosen ostracode fossils as our primary indicator because they have proven to be extremely useful in the reconstruction of lacustrine paleoenvironments, through their rapid response (in the form of changing species composition, abundance and diversity) to climate-related limnologic change (see *e.g.* Palacios-Fest *et. al*, 1994; Holmes and Chivas, 2002; Forester, 1983,1985,1986,1987,1991a,1991b; Forester and Brouwers, 1985; Smith, 1993a,1993b; Smith, et al. 1992). Other fossil invertebrates were also used as paleoecological indicators in this study. Both brine shrimp and brine fly fossils are excellent indicators of hypersaline environments because they have a much higher salinity tolerance than most other invertebrates. Brine shrimp (*Artemia* salina) fossils are in the form of egg capsules, fecal pellets and occasionally chitinous exoskeletal fragments. Brine fly larvae (*Ephydra riparia*) are abundantly preserved as highly sclerotized proleg claws, or less commonly as intact larvae, adults or exoskeletal fragments. Lastly, freshwater molluscs were used as indicators of marsh or shallow littoral environments. *Physella* spp. and various species of planorbid gastropods were found in many horizons.

Samples were taken from the GSL-004 core at 1 meter intervals to supplement the core catcher samples obtained during the August 2000 drilling operation. We disaggregated, cleaned and processed all core samples using a variant of Forester et al (1994). Using a 125-micron sieve, we separated the ostracodes and coarser sediments from the finer material. The >125-micron fraction was oven dried at 40°C and weighed. Micropaleontologic and sedimentary indicators were visually estimated as percent per sample using Olympus SZX12 and Leica MZ12 stereo microscopes. Micropaleontologic indicators include ostracodes, brine shrimp fossils, brine fly fossils, gastropods, and bivalves. Sedimentary indicators include quartz grains, mafic and other terrigenous sediments and pyrite. Samples that contained a high abundance of ostracodes and/or brine shrimp fossils were sub-sampled and counted. The dry weights of both the subsample and the sample were used to estimate number/gm. In samples that had low abundance of ostracodes all were counted, otherwise, ostracodes were counted to 300 individuals. Both juveniles and adults were counted, but only adults/sub-adults were identified and used in our paleoecological interpretations. Identification was to the lowest possible taxonomic level, usually species, and was based on published sources (Delorme 1970a, 1970b, 1970c, 1970d, 1971, 1991), personal communication with Dr. Richard Forester of the USGS and Dr. Manuel Palacios-Fest of Terra Nostra Earth Science Research, and comparison with the University of Arizona lacustrine ostracode collection.

We used DCA (detrended correspondence analysis) to gain a better understanding of the temporal variability of ostracode assemblages throughout the core. This method of indirect gradient analysis arranges samples from the core containing ostracodes in multivariate space. Samples that cluster together have similar species compositions and samples that are separated in multivariate space have less similar compositions. Because

explicit (*i.e.* modern) ostracode-environmental data were not compiled, direct gradient analysis such as CCA (Canonical Correspondence Analysis) could not be used. Therefore, the significance of multivariate axes must be inferred from our general knowledge of the distribution of these ostracode species (see *e.g.* Delorme 1970a, 1970b, 1970c, 1970d, 1971, 1991Palacios-Fest *et. al*, 1994; Holmes and Chivas, 2002; Forester, 1983,1985,1986,1987,1991a,1991b; Forester and Brouwers, 1985; Smith, 1993a,1993b; Smith, et al. 1992). To increase the robustness of our multivariate analysis, we applied the following constraints: (i) only ostracode taxa that had an abundance of 10 individuals/gm in at least one sample were included and (ii) samples had to contain at least 10 ostracodes/gm to be included. Ostracode percent data were arc-sin transformed prior to analysis, and analyzed using DCA with CANOCO 4 for WINDOWS. DCA plots were generated in CanoDraw and modified for clarity in Adobe Photoshop.

GEOCHRONOLOGY AND AGE MODEL

A robust age model is crucial to constrain the timing of environmental changes recorded by our paleontological and sedimentological indicators. Radiocarbon dates provide age constraints for sediments younger than ~30,000 cal yr B.P. ^{14}C AMS dating was only possible above the upper salt horizon , > 9 mblf (<12,500 cal yr B.P.) because there was no datable terrestrial material between the evaporite layer and the maximum depth (age) allowable for reliable radiocarbon dates. U-series geochronology was used to constrain the age of sediments older than 30,000 yr B.P. This dating method is commonly used in studies of Quaternary climate change because it can accurately date evaporite and aragonitic deposits beyond the limit of radiocarbon dating (e.g. Li et al. 1996; Lin et al. 1996). Two U-series dates were obtained for the preliminary study (Dean *et al.* 2002) and yielded preliminary

ages of 41,000 yr B.P. at 19 mblf and 231,000 yr B.P. at 95.6 mblf. The uppermost sample is constrained by the Hansel Valley Ash at 17.2 mblf (26,500 yr B.P.) and suggests that the U/Th dates may be maximum estimates. Material for new U-series dating came from the two thick evaporite layers found from 14.34 - 10.62 mblf and from 70.63 - 67.79 mblf.

^{14}C AMS Dating

Nine samples within the upper 12 meters contained material that could be used for radiocarbon dating. The material was primarily hand-picked charcoal, however, one sample was 150 μg of hand-picked leaf hairs (taxonomy unknown, but unquestionably from terrestrial plant families). The charcoal samples could not be accurately weighed before pretreatment because they were extremely small (< 50 μg). Samples were pretreated, combusted and processed at the AMS Laboratory at the University of Arizona. All samples were assumed to be of terrestrial origin, and therefore were not subjected to any reservoir corrections. We calibrated all radiocarbon dates to calendar years using Calib 4.4 (www.depts.washington.edu/qil/calib). If the radiocarbon age was beyond the range for tree ring calibration curves, we used a mean calibrated age calculated from two different calibration curves, one generated from stalagmite data and the other from Lake Suigetsu's annually laminated sediments (Beck *et al.* 2001; Kitagawa and van der Plicht, 1998).

U-series Dates

Material for the U-series dates came from evaporite deposits from two core horizons; core drives 4A-6A-1 (41cm, 11.89 mblf) and 4B-10A-1 (40cm, 68.11 mblf). ^{230}Th dates were obtained using thermal ionization mass spectrometry (TMS) (Chen *et al.*, 1986; Edwards *et al.*, 1987) by Larry Edwards and Hai Cheng at the University of Minnesota. Corrections were estimated using an upper constraint of the Hansel Valley ash (26.5 ka) and crustal

values for detrital contaminants. Isochron methods could not be used to calculate correction factors because variability in detrital ^{230}Th did not give an adequate plot on the isochron. For all U-series dates, we used ^{232}Th corrected values for our age model. Although corrected and uncorrected ages gave us similar results, the corrected values gave a more continuous estimate of ages between the two regressions (smaller gap in age estimates between the two regressions). Also, the corrected values gave consistently younger estimates, which are in better agreement with age estimates from other sources.

We excluded U-series dates that were obtained from an upper evaporite layer at 11.89 mblf. The corrected dates conflict with the very well documented date for the Mazama tephra and the uncorrected dates conflict with the well-supported chronology for the Lake Bonneville Highstand (Oviatt, 1997; Currey and Oviatt, 1985; Oviatt et al., 1992; Spencer et al., 1984 among others).

Tephra and Biostratigraphic Correlation

Two tephra layers have been positively identified in the core. The Mazama Ash is located 4.77 mblf and has a published age of 7627±150 cal yr BP, which is very well constrained (Zdanowicz *et al.* 1999). The Hansel Valley Ash appears 17.2 mblf and has a published age of 31288±127 cal yr BP (Oviatt et al. 1992).

We used biostratigraphic correlations for two age constraints on horizons 13.31 and 15.79 mblf. Our correlation at 15.79 mblf used an assemblage containing the ostracode species *Candona adunca* and *Limnocythere ceriotuberosa*, an assemblage that has, to date, only been associated with the middle transgressive phase of Lake Bonneville, dated in other deposits at 15860±180 ^{14}C years (18718 ± 290 cal yrs BP) (Thompson *et al*, 1990; Oviatt *et al.* 1992).

At 13.31 mblf, after the Bonneville Highstand deposits, the only invertebrate fossils present in our core sample are brine shrimp egg capsules. This is consistent with other shoreline and core evidence, which indicates that after the Bonneville Highstand, egg capsules appear in the fossil record before brine shrimp pellets (Dr. Jack Oviatt of Kansas State University, personal communication, 2003). We correlated our brine shrimp egg capsules with the bottom of unit IIIa in the core studied by Thompson et al. (1990). The bottom of unit IIIa was deposited after Bonneville Highstand and is right below the appearance of brine shrimp pellets at 12,100 $\pm$ 130 ^{14}C yr B.P. (14,091$\pm$ 283 cal yr B.P.).

Our age model uses a combination of dates generated by C^{14} and U-series dating, plus the constraints provided by the biostratigraphic correlations discussed above (see Table 1). Because the dated material is not evenly dispersed throughout the core, we generated our age model using a split-regression. We used a non-linear, third order polynomial regression for the upper portion of the core (< 19 mblf). This provided age estimates that were most consistent with the very constrained, well-documented Mazama and Hansel Valley tephra dates, and is consistent with: (*i*) expected faster sedimentation rates during the Pleistocene/Holocene boundary evaporite deposition and (*ii*) slower sedimentation rates in the less compacted core top sediments. The age model for the bottom part of the core was generated with a linear regression because the dates in the lower portion of the core are not as constrained as in the upper part of the core. Also, a linear regression reduced the gap between the split regressions, allowing a more continuous estimate of ages.

RESULTS

Lithofacies

The lithofacies of GSL00-4 are shown in figure 4. The lithostratigraphy of GSL00-4 was analyzed by Doug Schnurrenberger and Brian Haskell at the Limnological Research Institute at the University of Minnesota (Dean *et al.* 2002). Starting at the base of the core, they found that the bottom 3 meters of GSL00-4 are variegated and gray laminated carbonate muds. Above these muds, beginning around 117 mblf, are massive to laminated clayey sands, brownish silts and pale green muds that are mottled and show evidence of bioturbation. Our micro-sedimentological core samples indicate abundant pyrite in this unit along with fluxes of quartz grains. From 105 to 97 mblf, massive mottled pale green muds and intensively mottled brown intervals containing cracks dominate the lithology. Above this unit, from 97 - 70 mblf, are intervals of banded, cm-bedded, or finely laminated dark gray, green and gray carbonate muds and silts, sometimes diatomaceous. Also, some sandy laminae and dolomite muds are present. There is no/little pyrite but quartz grains are abundant in some horizons. The upper part of this unit, from 74 to 70 mblf, consists of laminated carbonate muds, some of which are diatom rich. The first of two evaporite layers appears from 70 to 67 mblf. It mainly consists of halite (NaCl) with some mud laminae. On top of the salt crust are gray - green carbonate muds containing cm-thick gypsum layers. Above 61 mblf, the gypsum disappears and terrigenous sediment grains, including quartz grains, become more abundant. Terrigenous sediments peak around 57 mblf, massive-banded gray silty muds and sandy layers dominate. The muds contain subaerial exposure features and some reddish algal rich laminae. Variegated and mottled carbonate muds appear around 54 mblf and contain dewatering structures, roots, soft sediment deformation,

pseudomicrokarst structures and faults. The lithology changes at 36 mblf to finely laminated variegated (gray, green and black) carbonate muds and clays, with some sandy and algal rich (diatomaceous) layers. The Hansel Valley ash is located at 17.20 mblf, within massive to finely laminated gray carbonate muds. One meter of black sapropelic muds appears around 15 mblf, which is immediately overlain by the upper, 3m thick evaporite layer.. This evaporite is mainly thenardite (Na_2SO_4)with mm- to cm- interbeds of black sapropelic mud. Above the upper salt crust, black sapropel muds containing salt crystals continue until 8.20 mblf. From 8.20 mblf to the top of the core, pelleted aragonite muds dominate the lithology.

Biofacies

The biofacies of GSL00-4 are shown in figure 5. Beginning at the bottom of the core, brine shrimp fecal pellets make a brief appearance in the fossil record but brine fly fossils are most common. Ostracodes make their first appearance with a monospecific assemblage of *Limnocythere staplini*, an indicator of high salinity, at 120 mblf, but then quickly disappear. *L. staplini* reappears at 112 mblf, and brine fly fossils disappear within the same horizon. Ostracodes become abundant at 107 mblf when an assemblage dominated *by L. staplini* and *Candona patzcuaro,* a halotolerant species, appear. Ostracode diversity increases in the next 2 meters to include species common to marshes, such as *Cyprideis beaconensis* and *Cyprideis salebrosa*. Many of the ostracode carapaces are reduction stained. Coexisting with this group of ostracodes are molluscs, particularly gastropods. Above 97 mblf, ostracodes disappear and brine flies increase in abundance. Gastropods disappear too except for a brief sandy interval from 91-90 mblf. *L. staplini* becomes abundant briefly once again at 81 mblf, but then disappears until 72 mblf. At 71.5 mblf, we found two adult *Candona* spp. individuals in good/fair taphonomic condition, indicative of freshwater conditions. From 70

- 61.44 mblf, there are no fossils except a very small number of brine shrimp fecal pellets. Ostracodes are present, in low numbers, from 57- 52 mblf, but become highly diverse from 52 - 40 mblf. This assemblage includes *L. staplini, C. beaconensis, C. patzcuaro, Heterocypris* spp.(common marsh species), *Cypridopsis vidua* (groundwater species), *L. friabilis*, and *L. ceriotuberosa* (both of which prefer cool, less saline water). Molluscs are also abundant in this interval. By 49 mblf, only *L. staplini and C. vidua* remain in the record, but they disappear shortly thereafter. An assemblage dominated by *L. platyforma* (freshwater ecophenotype of *L. ceriotuberosa*) and *L. friabilis* occurs briefly around 45 mblf. The only fossils found between 44 -16 mblf are brine flies and occasional *L. staplini*. At 16.59 mblf, an assemblage of *L. staplini* and *Candona* (cf.) *caudata* occurs. Ostracodes are very abundant in this zone. Directly above this, at 15.79 mblf, we found abundant *Candona adunca* and *L. ceriotuberosa,* indicative of freshwater conditions. Above the upper evaporite layer (14.34 mblf), brine shrimp egg capsules are the first fossils to appear, followed by brine fly fossils and abundant brine shrimp fecal pellets. The only ostracodes recovered above the upper salt horizon were reworked specimens.

Multivariate Analysis

Figure 6 presents the DCA results for the ostracode species and samples that qualified for the multivariate analysis (see Table 3). DCA major axes 1 and 2 account for 28.4 and 17.4% of the total variance, respectively. DCA plots for species and samples suggest that Axis 1 represents a salinity gradient and Axis 2 may represent a vegetation or lake level gradient, however a more robust analysis that includes environmental data is needed. The ordination plot shows three fairly distinct assemblages: (i) fresh open-water indicators, dominated by *Candona* spp. (ii) saline open-water indicators, dominated by *L. staplini*; (iii)

salt or freshwater marsh indicators, dominated by a high diversity of ostracodes including *Cyprideis beaconensis*, *C. salebrosa*, *Candona patzcuaro*, *Cypridopsis vidua*, *Heterocypris* spp., *Potamocypris unicaudata*, *Cyclocypris* spp, *Limnocythere ceriotuberosa* and *L. friabilis*). The assemblages are mutually exclusive, only one assemblage is present at any time. The dominant assemblage fluctuates in multivariate space mainly between the 'marsh indicators' and the 'saline open-water indicators', the 'fresh open-water indicators' rarely appear (see arrows in Fig.6). This suggests that the environment at the core site through time has fluctuated mostly between shallow saline water and marsh conditions, with open fresh water events being extremely rare.

Biofacies and Lithofacies Zonation and Paleoenvironmental Significance

We have combined similar and contiguous lithofacies and biofacies , as well as the results of our ostracode multivariate analysis into a series of stratigraphic zones (see Figs 4 and 5.). These zones are represented by a particular depth interval and an age based on our core geochronology (Figs 2 and 3). The zones elucidate the systematic environmental changes that have occurred at the GSL00-4 core site over the last 240,000 yr B.P.

Zone A: 121 - 117 mblf (241,200 - 235,000 yr B.P.)

This zone begins as a saline open water environment as suggested by its gray/variegated muds with fine laminations and the presence of *Limnocythere staplini* (in low abundance), brine flies and brine shrimp. Fine laminations indicate slow deposition rates and a lack of bioturbation, which are common in calm, deeper water. *Limnocythere staplini* disappear by 239,000 yr B.P. and only brine fly and brine shrimp fossils remain throughout the rest of the zone. This change in biofacies may indicate a switch from saline to

hypersaline conditions since brine flies and brine shrimp have a much higher salinity tolerance than *L. staplini*.

Zone B: 117 - 97 mblf (235,000 - 195,000 yr B.P.)

This zone shows evidence of a marginal lake environment based on the presence of mottled/bioturbated muds and sandy intervals, which indicate a higher energy level similar to the one found along lake shorelines, as opposed to the calmer and deeper water of a lake's profundal zone. Pyrite formation and reduction stains on ostracode carapaces are common in the reducing environment of marsh muds. Also, a high diversity of ostracodes and molluscs common to lake littoral zones are found from 107 - 99 mblf (215,000 - 198,000). Ostracode DCA analysis clusters samples from this zone in the 'marsh' assemblage. They are highly diverse and abundant when they appear in this interval, however, their stratigraphic record is sporadic throughout this interval. This may be caused by lake levels occasionally regressing below the core site as suggested by lithological characters such as brown-colored intervals with cracks and intense mottling indicative of soil formation.

Zone C: 97 - 70 mblf (195, 000 - 141,700 yr B.P.)

Most of this zone is indicative of saline to hypersaline, open lake conditions, based on the finely laminated muds and abundant brine fly fossils. Ostracodes are sparse this zone, however a couple of horizons (81mblf: *163,500 yr B.P* and 72 mblf: *144,700 yr B.P.*) contain abundant *L. staplini*. . Because of this, the ostracode DCA analysis clustered samples from this zone in the 'saline open-water' assemblage, even though we have evidence that other environments may have occurred in this zone. For instance, a brief sandy interval containing gastropods and a very low abundance of marsh ostracodes, along with the disappearance of brine fly fossils (91-90 mblf: 183,900 - 181,900 yr BP) may represent a short period when

lake level regressed and the core site was, once again, in a marsh environment. Also, at 71.5 mblf (143,500 yr B.P.), the presence of *in-situ* freshwater ostracode, *C. caudata*, within finely laminated variegated muds may indicate a brief period of open fresh water conditions towards the top of this zone.

Zone D: 70 - 61.44 mblf (141,700 - 122,800 yr B.P.)

Zone 'D' is dominated by indicators that suggest highly evaporative lake conditions. An authigenic evaporite unit from 70 - 67mblf (141,700 - 135,000 yr B.P.), lying immediately above the previously mentioned indications of relatively freshwater, open lake conditions indicates rapid desiccation and the presence of an extremely hypersaline lake that has reached the precipitation point of halite. No fossils occur in this zone except a very low abundance of brine shrimp fecal pellets. This combined with high $CaCO_3$ concentrations (mainly aragonite), and very low magnetic susceptibility indicates very dry and warm conditions.

Zone E: 61.44 - 35.89 mblf (122,800 - 71,600 yr B.P.)

Between 61 -57 mblf (123,000 - 114,900 yr B.P.) laminated muds with sandy intervals suggests small oscillations in lake level with the laminated muds being deposited in calmer, deeper water and sandy intervals in higher energy shoreline environments. Ostracodes appear in low abundance at this depth/time, except for 58 mblf (116,800 yr B.P) when abundant L. staplini appears briefly. From 57 -55 mblf (114,900 - 110,800 yr B.P.) subaerial exposure features at the top of a dm-thick fining upward sequence in the carbonate muds may indicate a brief period when the core site was terrestrial. Deposited on top of this, at 55 -54 mblf (110,800 - 108,900 yr B.P.) are laminated muds with sandy layers and no mottling which may signal a time when lake level increased and the core site was submerged

again. The core site reverted back to marsh conditions during the rest of the zone from 54 - 36 mblf (108,900 - 73,600 yr B.P.), with the lake level lying slightly below the core site as suggested by the presence of marsh ostracodes, molluscs and mottled carbonate muds containing roots, dewatering structures and soft sediment deformation. One horizon, 45 - 44 mblf (90,900 - 88,800 yr B.P.), may suggest groundwater discharge runoff maintained the marsh environment due to the presence of a freshwater assemblage of ostracodes, *L. friabilis* and *L. platyforma*, a freshwater ecophenotype of *L. ceriotuberosa*. Although the lithofacies and biofacies of this zone indicate predominantly marsh conditions, there is one interval, (48 - 46 mblf (96,900 - 92,700 yr B.P.), that indicates the site was periodically inundated by hypersaline lake water. This interval contains no/very few ostracodes, but contains abundant brine shrimp fecal pellets, brine shrimp egg capsules and brine fly fossils that are deposited in mm- to cm- laminated variegated muds.

Biofacies show a shift from marsh conditions to saline open-water conditions earlier than the lithofacies in this zone. The ostracode multivariate analysis clusters samples for Zone E as a 'marsh' assemblage, until 43 mblf (87,600 yr B.P.) when it shifts to a saline open-water assemblage. At this same depth/time, gastropods disappear and brine fly fossils become abundant. The lithostratigraphy, however, indicates that marsh conditions continue until 36 mblf (~73,600 yr B.P.). This apparent inconsistency may be a result of lithofacies and biofacies responding to different physical, chemical and biological signals within the environment.

Zone F: 36 - 14 mblf (71,600 - 17,000 yr B.P.)

Much of this zone shows evidence of a hypersaline lake as indicated by the combined presence of finely laminated gray and variegated muds and abundant brine fly fossils. *L.*

staplini is abundant between 30 - 28 mblf (61,000 - 57,000 yr B.P) and suggests the lake freshened from hypersaline to saline conditions. Between 28 and 16.59 mblf (57,000 – 23,000 yr B.P.) the lake fluctuates between saline and hypersaline conditions. This is indicated by the alternation between brine fly /brine shrimp fossils and *L. staplini* throughout the stratigraphic record for this interval. Our multivariate analysis indicates a shift from 'saline open-water' assemblages to 'fresh open-water' assemblages starts to take place by 16.59 mblf (23,500 yr B.P.) when *C.* (c.f.) *caudata* and *L. staplini* become abundant. *L. staplini* is not a salinity indicator in this case because it has very broad salinity tolerances and can survive in freshwater lakes. It is a salinity indicator only when it is found alone because it can withstand much higher salt concentrations than any other North American ostracode. DCA results indicate full deep freshwater conditions by 15.79 mblf (21,000 yr B.P.) with an assemblage of abundant *Candona adunca* and *L. ceriotuberosa*. Our regression-based age model assigns this interval an age that is slightly older than expected. We expected the date for this freshwater interval to be closer to the constrained age, 18,718 $\pm$ 290 yr B.P, based on biostratigraphic correlation (see Methods section). After the fresh open-water conditions, we have no ostracode record and black sapropelic muds may indicate a rapid decline in lake level because anoxic conditions are common in shallow water containing high salt concentrations. The black sapropelic muds are not fossiliferous.

Zone G: 14 - 0 mblf (17,000 - 0 yr B.P.)

The presence of the upper salt (thenardite) layer indicates another rapid desiccation event followed by hypersaline conditions and authigenic evaporite precipitation. Black sapropelic muds on top of the salt crust and later, pelleted aragonitic muds with the exclusive

presence of brine shrimp and brine fly fossils suggest the lake has remained hypersaline throughout the Holocene.

DISCUSSION

In zones A-G, we see frequent alternations in lithofacies and biofacies between (a) saline/hypersaline open water indicators, (2) salt or freshwater marsh indicators, or (3) open (deep) freshwater indicators. These alternations provides strong evidence for fluctuating lake levels at the core site, and by extension, regional paleohydrology and climatic conditions. However, these cannot be interpreted simply as a sequence of wetter (3) to drier (1) conditions, as might be expected. To understand this fact it is instructive to consider the lateral facies variations observed around the Great Salt Lake today. Surrounding the current saline lake are numerous freshwater, spring or seepage fed marshes, forming at the groundwater discharge zone along the lake margin. Frequent small scale fluctuations in lake levels cause these marsh sites to be either flooded by the saline lake during rising lake levels, or converted into erosional or soil forming surfaces when the lake level falls and the marshes migrate basinwards. Thus, a vertical sequence of sediments representing a transition from highest lake levels to lowest in this context is represented by a) deep water deposits and relatively freshwater indicators, to b) shallower, but still open, saline lake indicators, when the site is still fully submerged to c) saline marsh (lake margin) indicators as the site approaches the lake surface level, to d) freshwater marsh indicators (lake level slightly below core site, spring or fluvial discharge), to e) paleosols and erosion surfaces when lake level is well below the core site (Fig. 7). Similarly, evaporite deposits should not be thought of as representative of the lowest/driest lake conditions. More probably they form at times when the large dissolved solid budget of a large and deep lake is undergoing its most rapid brine

concentration. Textural evidence from the GSL00-4 core evaporates also suggests they formed subaqueously, analogous to the salts of rapidly concentrating brines in other ancient and modern hypersaline lakes (e.g. Li et al. 1996; Krumgalz, 1997). The volume/thickness of evaporite sequences in the Great Salt Lake is therefore strongly linked to the volume of the antecedent waterbody; lower preceding high-stands will yield smaller evaporite bodies upon evaporite precipitation.

GSL00-4 and Global Climate Change

General Circulation Models (GCMs) have predicted that a southward diversion of the jet stream during glacial maxima would have a major impact on precipitation/evaporation ratios in the eastern Great Basin (COHMAP, 1988; Thompson *et al.* 1993). The record of lake level oscillations contained in GSL00-4 is in agreement with GCMs predictions and show that the system has been strongly influenced by climate forcing over the last three glacial/interglacial sequences. We have compared the marine OIS chronology (Martinsen *et al.* 1987) with the timing of local lake oscillations and have confirmed that the pattern of paleohydrological change recorded in the sediments of GSL00-4 was largely controlled by global changes in climate (Fig.8).

OIS 7 (241,000 – 189,000 yr B.P.)

Although lake levels oscillate considerably during this stage, they overall tend to decrease. Close to the beginning of this interglacial, at 241,000 yr B.P., the basin contained an shallow saline lake (zone A, bottom) but soon after the water became hypersaline (zone A, top). This does not necessarily indicate that lake level decreased, it just suggests a higher brine concentration. However, there are good indications that evaporation was causing lake levels to decrease overall because by 235,000 yr B.P. (stage 7.4), lake levels were at/below

the core site and marsh conditions were dominant (zone B). Periodic soil formation (zone B 211,000 – 195,000 yr B.P.) correlates with the highest (warmest) peak in stage 7. Lake levels began to rise and inundate the core site by 195,000 yr.B.P. and by the end of stage 7, the lake level was higher and hypersaline (zone C, bottom).

OIS 6 (189,000 – 129,700 yr B.P.)

Lake levels fluctuate primarily between saline and hypersaline conditions throughout this glacial cycle. However, water levels drop to the core site during the brief marsh interval in zone C (183,900 – 181,900 yr B,P), which correlates with late OIS 6.5, the highest peak in this cycle. Transgression of lake levels from shallow saline to deep freshwater by 143,000 yr B.P is suggested by the *in-situ* freshwater ostracodes found in zone C. The age of this potentially deep freshwater lake correlates with the timing of the Little Valley Highstand complex (~150,000 yr B.P) based on amino acid dating of gastropod shells from a lacustrine sand in Little Valley (Scott *et al.* 1983; Oviatt *et al.* 1999). At our level of resolution, the lower evaporite (halite) layer (zone D) was deposited immediately following the lake highstand during OIS 6.2. This slightly contradicts the GCM's prediction because OIS 6.2 should have been close to the maximum extent of the North American ice sheet and therefore, brought greater precipitation (not evaporation) to the area. We belive it is more likely that the evaporite layer was deposited close to the OIS6/OIS5 transition, and that the age discrepancy is most likely due to the lack of age constraints in the lower portion of our age model.

OIS 5 (129,700 – 73,910 yr B.P.)

From OIS 5.5 to the middle of OIS 5.4, (123,000 – 114,900 yr B.P.) many small lake level oscillations occur in the basin causing an alternation in environments at the core site

from shallow saline to hypersaline conditions. Lake level decreases to the point of subaerial exposure at the core site from 114,900 – 110,800 yr B.P. (zone E). Lake levels increase slightly by 108,900 yr B.P. but remain at/slightly below the core site for the remainder of this interglacial stage as indicated by the extreme marsh conditions at the core site (zone E). As mentioned previously, the lithofacies and biofacies shift out of phase with one another in this zone. GSL00-4 biofacies indicate a shift from marsh conditions to a shallow saline lake around 87,600 yr B.P., close to the interglacial peak at OIS 5.1. However, lithofacies show this environmental transition occurring later, at the OIS 5/OIS4 transition. It is possible that the biology of the system is more sensitive to climate driven limnological variations and therefore, responds earlier to environmental changes than the geological record.

OIS 4 (73, 910 –58,960 yr B.P.)

The environmental conditions at the core site throughout most of this glacial cycle were, in large part, hypersaline (zone F). However, abundant *L. staplini* from 61,000 – 57,000 yr B.P. suggest that lake level increased to open saline conditions around the OIS 4/OIS 3 transition. The age of this saline lake correlates with the published age of 59,000 $\pm$ 5000 yr B.P. for the Cutler Dam Alloformation (Kaufman et al. 2001). Our results suggest that the Cutler Dam Highstand did not include a deep freshwater interval, which is consistent with shoreline studies that indicate the Cutler Dam shoreline is at an elevation significantly lower than the Bonneville or Little Valley shorelines (Kaufman *et al.* 2001, Oviatt *et al.* 1999). The lower magnitude of OIS 4 glaciation brought less precipitation to the basin and therefore, lower lake levels than those associated with either the stage 6 (Little Valley) or the stage 2 (Bonneville) glaciations (Kutzbach *et al.* 1994; Kaufman *et al.* 2001). Our study is in agreement with Kaufman et al. (2001) who indicated that, like the Bonneville Highstand,

the maximum highstand for Cutler Dam occurred following a peak in global glacial stage (see Fig.8).

OIS 3 (58,960 – 24,110 yr B.P.)

Throughout this interglacial, lake levels remained fairly low and oscillated between shallow saline and hypersaline conditions at the core site (zone F).

OIS 2 (24,110 – 12,050 yr B.P.)

GSL00-4 records the presence of a deep freshwater lake in the basin from 23,500 – 21,000 yr B.P. (stage 2.2). The *C. adunca/L.ceriotuberosa* assemblage in zone F, correlates this deep freshwater lake to the middle transgressive phase of Lake Bonneville (Oviatt *et al.* 1992). Oviatt *et al.* (1992) constrained the age of this phase as occurring between 20,000 – 18,000 yr B.P., this is more robust age estimate than the slightly older date predicted by our age model.

The upper evaporite (thenardite) layer (zone G) was deposited sometime between 16,700 – 12,000 yr B.P. according to our age model. This is consistent with the post-Provo regressive phase of Lake Bonneville when, at 14,000 yr B.P., overflow ceased following the Bonneville Flood and the basin became hydrologically closed once again (Oviatt et al. 1992).

OIS 1 (12,050 – 0 yr B.P.)

Since the early Holocene, lake levels have remained low and hypersaline conditions have prevailed in the Great Salt Lake basin. Our study was at too low of a resolution to capture the Gilbert shoreline complex or any of the small lake level oscillations that are discussed in Currey (1990).

Conclusion

GSL00-4 contains a highly resolved paleoecological record of Quaternary environmental and climate change, and our intermediate resolution sampling (~2,000yr) of this record is a first step in unlocking the rich paleoenvironmental story of the Bonneville basin recorded here. Its paleoecological and sedimentological indicators show that the core site has fluctuated over time between marsh and saline open-water conditions, but has, on occasion, been submerged in deep fresh water. These local environmental changes can be understood in terms of oscillating lake levels. Our study confirms that climate forcing has played a major role in these lake level fluctuations. Overall, we see low to very low lake levels during the interglacial cycles (OIS 7, 5 , 3 and 1). The lowest lake levels coincide with the presence of marsh indicators in the core's sedimentary and paleoecological record. Saline/hypersaline conditions at the core site indicate regional lake levels higher than lake levels during marsh phases, but significantly lower than open freshwater conditions, such as the Little Valley cycle (late OIS 6) and the Lake Bonneville cycle (late OIS 2). Many smaller lake level oscillations are recorded in GSL00-4, however this study was at too low a resolution to describe these fluctuations in detail. With higher resolution sampling and a more robust age model, we may find that these smaller oscillations are sensitive to climate changes on millennial or shorter time scales. Oviatt (1997) found that some of the lake fluctuations associated with Lake Bonneville coincided with millennial scale Heinrich events.

The sediments contained in GSL00-4 provide a detailed natural archive of (1) local environmental and ecological change at the core site (2) fluctuations in regional paleohydrology and (3) climate change over the last three glacial/interglacial sequences.

This long, continuous record provides important insights into the paleoecology, paleohydrology and paleoclimate of the northeastern Great Basin, and will allow us the unique opportunity to link these insights into an interdisciplinary framework of past global change.

Acknowledgements:

The authors wish to gratefully acknowledge several people. A special thanks to DOSECC and their drilling crew, for without them, this study would not exist. We also wish to thank Rick Forester and Manuel Palacios-Fest for invaluable help with ostracode taxonomy and ecology; Doug Schnurrenberger for his very helpful assistance with GSL00-4 core samples and information; Jack Oviatt, Owen Davis and Karl Flessa for their expertise and very helpful comments; Warren Beck and Todd Lange for their assistance with carbon dating; Larry Edwards and Hai Cheng for the use of their U-series dates; Karen Bossenbroek for her work on brine fly prolegs; and Kaustuv Roy for his constant support and use of his lab facilities during the Summer 2002; This research was generously supported by NSF grant ESH-9915068 to A.C. and a Summer 2002 internship to D.B. provided by DOSECC Inc.

REFERENCES

Antevs, E. (1948). Climatic changes and pre-white man. In "The Great Basin, with Emphasis on Glacial and Postglacial Times". *Bulletin of the University of Utah* 38, 167-191.

Beck, W.J., Richards, D.A., Edwards, R.J., Silverman, B.W., Smart, P.L., Donahue, D.J., Hererra-Osterheld, S.H., Burr, G.S., Calsoyas, L., Jull, A.J.T. and Biddulph, D. (2001). Extremely large variations of atmospheric ^{14}C concentration during the last glacial period. *Science* **292**, 2453-2458.

Chen,J.H., R.L. Edwards and Wasserburg, G.J. (1986). ^{238}U, ^{234}U and 232Th in seawater. *Earth Planet. Sci. Lett.* **80**, 241-251.

Currey, D.R. (1990). Quaternary palaeolakes in the evolution of semidesert basins, with Special emphasis on Lake Bonneville and the Great Basin, U.S.A. Palaeogeography, Palaeoclimatology, Palaeoecology **76**, 189 – 214.

COHMAP (1988). Climate changes in the last 18,000 years: observations and simulations. *Science* **241**, 1043-1052.

Currey, D.R. and Oviatt, C.G. (1985). Durations, average rates, and probable causes of Lake Bonneville expansions, still-stands, and contractions during the last deep-lake cycle, 32,000 to 10,000 years ago. *In*: " Problems of and Prospects for Predicting Great Salt Lake Levels" (P.A. Kay and H.F. Diaz, Eds), pp. 9 -24 Cent. Publ. Affairs Admin., Univ. Utah.

Davis, O.K. (1998). Palynological evidence for vegetation cycles in a 1.5 million year pollen record from the Great Salt Lake, Utah, USA. *Palaeogeog., Palaeoclim., Palaeoecol.* **138**, 175-185.

Davis O.K. and Moutoux, T.E. (1998). Tertiary and Quaternary vegetation history of the Great Salt Lake. *Jour. Paleolim.* **19**, 417-427.

Dean, W., Rosenbaum, J., Haskell, B., Kelts, K., Schnurrenberger, D., Valero-Garces, Blas, Cohen, A., Davis, O., Dinter, D. and Nielson, D. (2002). Progress in global lake drilling holds potential for global change research. *EOS Transactions, American Geophysical Union* **83**, 85,90-91.

Delorme, L.D. (1970a). Freshwater ostracodes of Canada, part I. Subfamily Cypridinae. *Canadian Journal of Zoology* **48**, 153-168.

Delorme, L.D. (1970b). Freshwater ostracodes of Canada, part II. Subfamilies Cypridopsinae and Herpetocypridinae, and family Cyclocyprididae. *Canadian Journal of Zoology* **48**, 253-266.

Delorme, L.D. (1970c). Freshwater ostracodes of Canada, part III. Family Candonidae. *Canadian Journal of Zoology* **48**, 1099-1127.

Delorme, L.D. (1970d). Freshwater ostracodes of Canada, part IV. Families Ilyocyprididae, Notodromadidae, Darwinulidae, Cytherideidae, Entocytheridae. *Canadian Journal of Zoology* **48**, 1251-1259.

Delorme, L.D. (1971). Freshwater ostracodes of Canada, part V. Families Limnocytheridae, Loxoconchidae. *Canadian Journal of Zoology* 49, 43-64.

Delorme, L.D. (1991). Ostracoda. *In* "Ecology and Classification of North American Freshwater Invertebrates" (Thorp, J.H. and Covich, A.P. Eds.) pp.691-721. Academic Press, San Diego.

Edwards,R.L., Chen,J.H., Ku, T.L., and Wasserburg, G.L. (1987). Precise timing of the Last Interglacial Period from Mass Spectrometric determination of Thorium -230 in Corals. *Science* **236**, 1547-1553.

Forester, R.M. (1983). Relationship of two lacustrine ostracode species to solute composition and salinity: implications for paleohydrochemistry. *Geology* **11**, 435-438.

Forester, R.M. (1985). Limnocythere bradburyi n.sp.: A modern ostracode from Central Mexico and a possible Quaternary paleoclimatic indicator. *Jour. Paleontology* **59**, 8-20.

Forester, R.M. (1986). Determination of the dissolved anion composition of ancient lakes from fossil ostracodes. *Geology* **14**, 796-798.

Forester, R.M. (1987). Late Quaternary paleoclimate records from lacustrine ostracodes. *In*: "North America and adjacent oceans during the last deglaciation" Vol. K-3 (Ruddima, W.F. and Wright, H.E. Ed.) pp. 261-276. Geol. Soc. of Am. Boulder, CO.

Forester, R.M. (1991a). Ostracode assemblages from springs in the western United States: Implications for paleohydrology. *Mem. Entomol. Soc. Canada* **155**, 181-201.

Forester, R.M. (1991b). Pliocene-climate history of the Western United States derived from lacustrine ostracodes. *Quat. Sci. Rev.* **10**, 133-146.

Forester, R.M. and Brouwers, E. M.(1985). Hydrochemical parameters governing the occurrence of estuarine and marginal estuarine ostracodes: an example from south-central Alaska. *Jour. Paleontology* **59**, 344-369.

Gilbert, G.K., (1890). "Lake Bonneville". U.S.Geological Survey Monograph 1 p. 438. US Printing Office, Washington, D.C.

Holmes, J.A. and Chivas, A.R. (eds.). 2002. *The Ostracoda: Applications in Quaternary Research*. Amer. Geophys. Union Geophys. Monogr. 313pp.

Kaufman, D.S.,Forman, S.L., and Bright,J. (2001). Age of the Cutler Dam Alloformation (late Pleistocene), Bonneville Basin, Utah. Quaternary Research **56**, 322-334.

Kowalewska, A., and Cohen, A.S.,(1998). Reconstruction of paleoenvironments of the Great Salt Lake Basin during the late Cenozoic. *Jour. of Paleolimnology* **20**, 381-407.

Kitagawa, H. and van der Plicht, J. (1998). Atmospheric radiocarbon calibration to 45,000 yr B.P.: late glacial fluctuations and comogenic isotope production. *Science* **279**, 1187-1190.

Krumgalz, B.S. 1997. Ion interaction approach to geochemical aspects of the dead sea. *In* "The Dead Sea: the Lake and its Settings", (Niemi, T.M., Ben-Avraham, Z. & Gat, J.R. Eds.), pp.145-160. Oxford Monographs on Geology and Geophysics 36. Oxford University Press, New York and Oxford.

Kutzbach, J. E., Guetter, P.J. , Behling,P.J. and Selin,R. (1994). Simulated climatic changes: results of the COHMAP climate-model experiments. *In* "Global climates since the last glacial maximum", (Wright, Jr., H.E., J. E. Kutzbach, T. I. Webb, W. T. Ruddiman, F. A. Street-Perrott & P. J. Bartlein, Eds.), pp. 24-93. University of Minnesota, Minneapolis.

Li, G., Andrews, J.E., Riding, R., Dennis, P. and Dresser, Q. (1996). Possible microbial effects on stable carbon isotopes in Hot Spring travertines. *Jour. Sed. Res.* **66**, 468-473.

Li, J., Lowenstein, T.K., Brown, C.B., Teh-Lung, K. and Luo, S. (1996). A 100 ka record Of water tables and paleoclimates from salt cores, Death Valley, California. *Palaeogeography, Palaeoclimatology, Palaeoecology* **123**, 179-203.

Lin, J.C., Broecker, W.S., Anderson, R.F., Hemming, S., Rubenstone, J.L. and Bonani, G. (1996). New 230^{Th}/U and 14C ages from Lake Lahontan carbonates, Nevada, USA, and a discussion of the origin of initial thorium. *Geochim. Cosmochim. Acta* **60**, 2817-2832.

Martinson, D.G., Pisias, N.G., Hays, J.D., Imbrie, J., Moore, T.C. and Shackleton, N.J. (1987). Age dating and the orbital theory of the ice ages: development of a high resolution 0 to 300,000 year chronostratigraphy. *Quaternary Research* **27**, 1-29.

Oviatt, C. G., McCoy, W.D., and Reider,R.G. (1987). Evidence for a shallow Early or Middle Wisconsin-age lake in the Bonneville basin, Utah. *Quaternary Research* **2**, 248-262.

Oviatt, C.G., Currey, D.R., and Sack, D. (1992). Radiocarbon chronology of Lake Bonneville, Eastern Great Basin, USA. *Palaeogeography, Palaeoclimatology, Palaeoecology* **99**, 225-241.

Oviatt, C.G. (1997). Lake Bonneville fluctuations and global climate change. *Geology* **25**, 155-158.

Oviatt, C.G.,Thompson,, R.S., Kaufman, D.S., Bright, J. and Forester, R.M. (1999). Reinterpretation of the Burmester Core, Bonneville Basin, Utah. *Quaternary Research* **52**, 180-184.

Oviatt, C.G. (2002). Bonneville Basin lacustrine history: The contributions of G.K. Gilbert and Ernst Antevs. *In*: "Great Basin Aquatic Systems History", Smithsonian Contributions to the Earth Sciences 33. (R. Hershler, D.B. Madsen and D.R. Currey, Eds.), pp. 121-129.Smithsonian Institution Press, Washington D.C.

Palacios-Fest, M., Cohen, A.S., and Anadon, P. (1994). Use of ostracodes as paleoenvironmental tools in the interpretation of ancient lacustrine records. *Rev. Espan. Paleontol.* **9**, 145-164.

Scott, W.E., McCoy, W.D., Shroba, R.R,, and Rubin, M. (1983). Reinterpretation of the exposed record of the last two cycles of Lake Bonneville, western United States. *Quaternary Research* **20**, 261-285.

Smith, A.J. (1993a). Lacustrine ostracodes as hydrochemical indicators in lakes of the north-central United States. *Jour. Paleolim.* **8**,121-134.

Smith, A.J.. (1993b). Lacustrine ostracod diversity and hydrochemistry in lakes of the northern Midwest of the United States *in* "Ostracoda in the Earth and Life Sciences" (McKenzie, K.G. and Jones, P.J. Eds.), pp. 493-500. Balkema, Rotterdam.

Smith, A.J., Delorme, L.D., and Forester, R.M. (1992). A lake's solute history from ostracodes: comparison of methods. *In* "Water Rock Interactions" (Kharaka and Maest Eds.) p. 677-680. Balkema, Rotterdam.

Spencer, R.J., Baedecker, M.J., Eugster, H.P., Forester, R.M., Goldhaber, M.B., Jones, B.F., Kelts, K., Mckenzie, J., Madsen, D.B., Rettig, S.L., Rubin, M. and Bowser, C.J. (1984). Great Salt Lake, and precursors, Utah: the last 30,000 years. *Contrib. Mineral. Petrol.* **86**, 321-334.

Thompson, R. S., Whitlock, C., Bartlein, P.J., Harrison, S.P., and Spaulding, W.G. (1993). Climatic changes in the western United States since 18,000 yr B.P. *In* " Global Climates Since the Last Glacial Maximum" (H. E. Wright, Jr., J. E. Kutzbach, T.

Webb, III, W. F. Ruddiman, F. A. Street-Perrott, P. J. Bartlein, Eds). pp. 468-513. University of Minnesota Press, Minneapolis.

Thompson, R. S., Toolin, L.J., Forester, R.M., and Spencer, R.J.(1990). Accelerator-mass spectrometer (AMS) radiocarbon dating of Pleistocene lake sediments in the Great Basin. *Palaeogeography. Palaeoclimatology. Palaeoecology.* **78**, 301-313.

Zdanowicz, C.M., Zielinski, G.A., and M.S. Germani, M.S. (1999). Mount Mazama eruption: Calendrical age verified and atmospheric impact assessed. *Geology* **27**, 621-624.

APPENDIX

Table 1. Dates used to generate age model.

Table 2. AMS 14C dates from the upper 12 meter of GSL00-4

Table 3. Samples and species used in multivariate analysis (DCA). (*) Indicates a sample that was recently found to contain reworked ostracodes. We strongly believe that removing this sample will not change the overall results of the analysis and the pattern will remain the same. Nevertheless, the sample will be removed and the data will be reanalyzed before submission.

Figure 1. Map of the Great Salt Lake. The 'star' shows the location of the drilling operation for core GSL00-4; lat: 41 07' 50,20" long: 112 33'46.48" water depth: 9.30 m (Figure adapted from Dean *et al.* 2002).

Figure 2. Age models generated for core GSL00-4. We used a combination of ^{14}C, U-series, tephra and biostratigraphic correlation dates. Please see text for specific information on the technique used to generate the models.

Figure 3. Detailed age model used in our study. We chose the model using corrected U-series dates for various reasons (please see text). Note that the age scale is very different for the upper and lower portions of the core. The arrow indicates a data point that is shared between the upper and lower graphs. It is a U-series date from 19 mblf.

Figure 4. Lithostratigraphy and zonation of GSL00-4. Lithostratigraphy was analyzed by Doug Schnurrenberger and Brian Haskel at University of Minnesota. Other lithological indicators were sampled from the core by the authors (D.B. and A.C). Zonation corresponds to the zones discussed in the text.

Figure 5. Paleoecology and zonation of GSL00-4. We quantified brine shrimp pellets, egg capsules, and ostracodes as number/gm sediment. We measured the quantity of brine fly parts, gastropods, bivalves and fish bones on a ratio scale of 'none', 'few' and 'many'.

Figure 6. Ordination plot from our multivariate analysis of the ostracode data. The arrows and letters indicate where/when major transitions took place between ostracode groups. A= earliest ostracode record in the core was found at 107.21 mblf,(~215,000 yr B.P.); it was a marsh assemblage; B= marsh assemblage disappeared at ~ 99.16 mblf (~198,000 yr B.P.) and gave rise to a saline open-water assemblage. Saline open-water assemblage disappears around 58.21 mblf (~116,000 yr BP), ostracodes in high abundance did not occur again until 52.20 mblf (104,700 yr B.P.) when a saline marsh assemblage appears. C= transition in marsh assemblage from salt marsh to freshwater marsh occurs at ~45 mblf (~90,000 yr B.P.). D= A transition back to saline open-water conditions happens at ~44.29 mblf (~88,800 yr B.P.). Lake conditions stay this way until a brief fresh open-water event occurs at ~16 mblf (~22,000 yr B.P.) E.

Figure 7. Cartoon showing core site in terms of regional lake level fluctuations. See text for discussion.

Figure 8. Comparison of GSL-4 zonation withSPECMAP (from Martinson *et al.* 1987). Bonneville, Cutler Dam, and Little Valley refer to specific horizons in the core where we believe high stand sediments were deposited.

Depth(mblf)	Method	Dates (U-series uncorrected)	Dates (U-series corrected)	Reference
2.95	carbon14 (charcoal)	6148±1642 cal yr BP	6148±1642 cal yr BP	Balch et al., unpublished data
4.77	tephra correlation (Mazama)	7627±150 cal yr BP	7627±150 cal yr BP	Zdanowicz et al., 1999
5.06	carbon14 (charcoal)	10209±3005 cal yr BP	10209±3005 cal yr BP	Balch et al., unpublished data
5.88	carbon14 (charcoal)	11381±3950 cal yr BP	11381±3950 cal yr BP	Balch et al., unpublished data
6.05	carbon14 (charcoal)	9873±3566 cal yr BP	9873±3566 cal yr BP	Balch et al., unpublished data
6.05	carbon14 (leaf hairs)	10747±3588 cal yr BP	10747±3588 cal yr BP	Balch et al., unpublished data
8.98	carbon14 (charcoal)	12545±4400 cal yr BP	12545±4400 cal yr BP	Balch et al., unpublished data
11.89	U-series	15550±1050 yr BP	5380±5380 yr BP	Edwards and Cheng, unpublished data
11.89	U-series	17470 ±890 yr BP	7180±5500 yr BP	Edwards and Cheng, unpublished data
11.89	U-series	16650±1000 yr BP	6150±1000 yr BP	Edwards and Cheng, unpublished data
13.31	biostratigraphic correlation	14091±283 cal yr BP	14091±283 cal yr BP	Thompson et al, 1990
15.80	biostratigraphic correlation	18718±290 cal yr BP	18718±290 cal yr BP	Thompson et al, 1990
17.20	tephra correlation (Hansel Valley)	31288± 127 cal yr BP	31288± 127 cal yr BP	Oviatt et al, 1992
19.00	U-series	41000±244 yr BP	30838± 5000 yr BP	Edwards and Cheng, unpublished data
68.11	U-series	197700±15500 yr BP	168900±21000 yr BP	Edwards and Cheng, unpublished data
68.11	U-series	164200±11000 yr BP	137500±17800 yr BP	Edwards and Cheng, unpublished data
68.11	U-series	197000±50000 yr BP	173000±40000 yr BP	Edwards and Cheng, unpublished data
68.11	U-series	170000±16800 yr BP	142600±21000 yr BP	Edwards and Cheng, unpublished data
95.60	U-series	230953±16000yr BP	123900±37800 yr BP	Edwards and Cheng, unpublished data
118.70	U-series	287085±15000 yr BP	250922±19000 yr BP	Edwards and Cheng, unpublished data

Table 1.

AA#	LAB#	SAMPLE ID	δC^{13}	^{14}C yr	cal yr BP
AA53602	T17311	GSL-2	M	5500 ± 740	6148 ± 1642
AA53605	T17314	GSL-5	M	8800 ± 1300	10209 ± 3005
AA53606	T17315	GSL-6	M	9600 ± 1300	11381 ± 3950
AA53607	T17316	GSL-7	M	8500 ± 1500	9873 ± 3566
AA53608	T17317	GSL-8	M	9300 ± 1500	10747 ± 3588
AA53609	T17318	GSL-9	M	10700 ± 1800	12545 ± 4400

Table 2.

HOLE ID	DCA #	DEPTH	AGE cal yr B.P.	OSTRACODES
4A-1H-CC	1*	3	6771	*Limnocythere staplini, (Candona patzcuaro, Cypridopsis vidua, Candona adunca)*
4E-2A-2	2	15.8	21152	*Candona adunca, Limnocythere ceriotuberosa*
4E-2A-CC	3	16.6	23492	*Limnocythere staplini, Candona (cf.) caudata*
4E-3H-CC	4	19.4	38872	*Limnocythere staplini, Candona (cf.) caudata, (Cypridopsis vidua,Limnocythere ceriotuberosa, Cyprideis beaconensis.Candona patzcuaro.*
4E-4H-CC	5	22.6	45294	*Limnocythere staplini*
4E-6H-CC	6	28.7	57595	*Limnocythere staplini*
4E-7H-1	7	29.7	59642	*Limnocythere staplini*
4E-7H-2	8	30.5	61107	*Limnocythere staplini*
4E-9H-CC	9	37.7	75597	*Cyprideis beaconensis, (Limnocythere staplini, Candona patzcuaro, Cypridopsis vidua)*
4E-10H-1	10	38.7	77699	*Limnocythere staplini, (Heterocypris* spp.*)*
4E-10H-2	11	39.7	79701	*Limnocythere staplini*
4B-1H-1	12	44.3	88882	*(Candona patzcuaro, Limnocythere platyforma, Limnocythere friabilis, Cyclocypris* spp.*, Heterocypris* spp.*)*
4B-1H-2	13	45.3	90904	*Limnocythere platyforma, (Limnocythere staplini, Limnocythere friabilis, Candona patzcuaro, Cyprideis beaconensis. Heterocypris spp.)*
4B-2H-CC	14	49.2	98695	*Limnocythere staplini, (Cypridopsis vidua, Candona patzcuaro, Cyprideis beaconensis, Cyclocypris* spp.*)*
4B-3H-2	15	50.3	100893	*Candona patzcuaro, Limnocythere staplini, Limnocythere friabilis (Cyprideis salebrosa,Heterocypris* spp.*, Limnocythere ceriotuberosa. Cypridopsis vidua)*
4B-3H-2	16	51.3	102920	*Limnocythere staplini, Candona patzcuaro, Heterocypris* spp.*(Limnocythere friabilis, Limnocythere ceriotuberosa. Cyprideis salebrosa. Potamocypris unicaudata)*
4B-3H-CC	17	52.2	104756	*Limnocythere staplini, Cyprideis beaconensis, Candona patzcuaro (Cypridopsis vidua, Potamocypris unicaudata)*
4B-5H-CC	18	58.2	116817	*Limnocythere staplini (Candona patzcuaro, Cyprideis beaconensis, Cypridopsis vidua)*
4B-11A-CC	19	72.2	144792	*Limnocythere staplini (Cypridopsis vidua, Candona patzcuaro, Cyprideis beaconensis)*
4C-3A-2	20	81.5	166205	*Limnocythere staplini*
4D-3A-2	21	98.2	197050	*Limnocythere staplini, Candona patzcuaro (Heterocypris* spp.*, Cyprideis salebrosa, Limnocythere friabilis, Limnocythere ceriotuberosa)*
4D-3A-CC	22	99.2	198996	*Limnocythere staplini, Candona patzcuaro, Cyclocypris* spp.*, Heterocypris* spp.*, Cypridopsis vidua, Cyprideis beaconensis (Cyprideis salebrosa. Potamocypris unicaudata)*
4D-4A-1	23	100.2	201071	*Limnocythere staplini, Candona patzcuaro, Limnocythere friabilis, Cyprideis salebrosa, Potamocypris unicaudata (Heterocypris* spp.*.. Cypridopsis vidua)*
4D-5A-CC	24	105.3	211238	*Cyprideis beaconensis, Limnocythere staplini (Candona patzcuaro)*
4D-6A-2	25	107.2	215141	*Candona patzcuaro (Limnocythere staplini, Limnocythere friabilis, Heterocypris* spp.*, Potamocypris unicaudata. Cypridopsis vidua)*

Table 3.

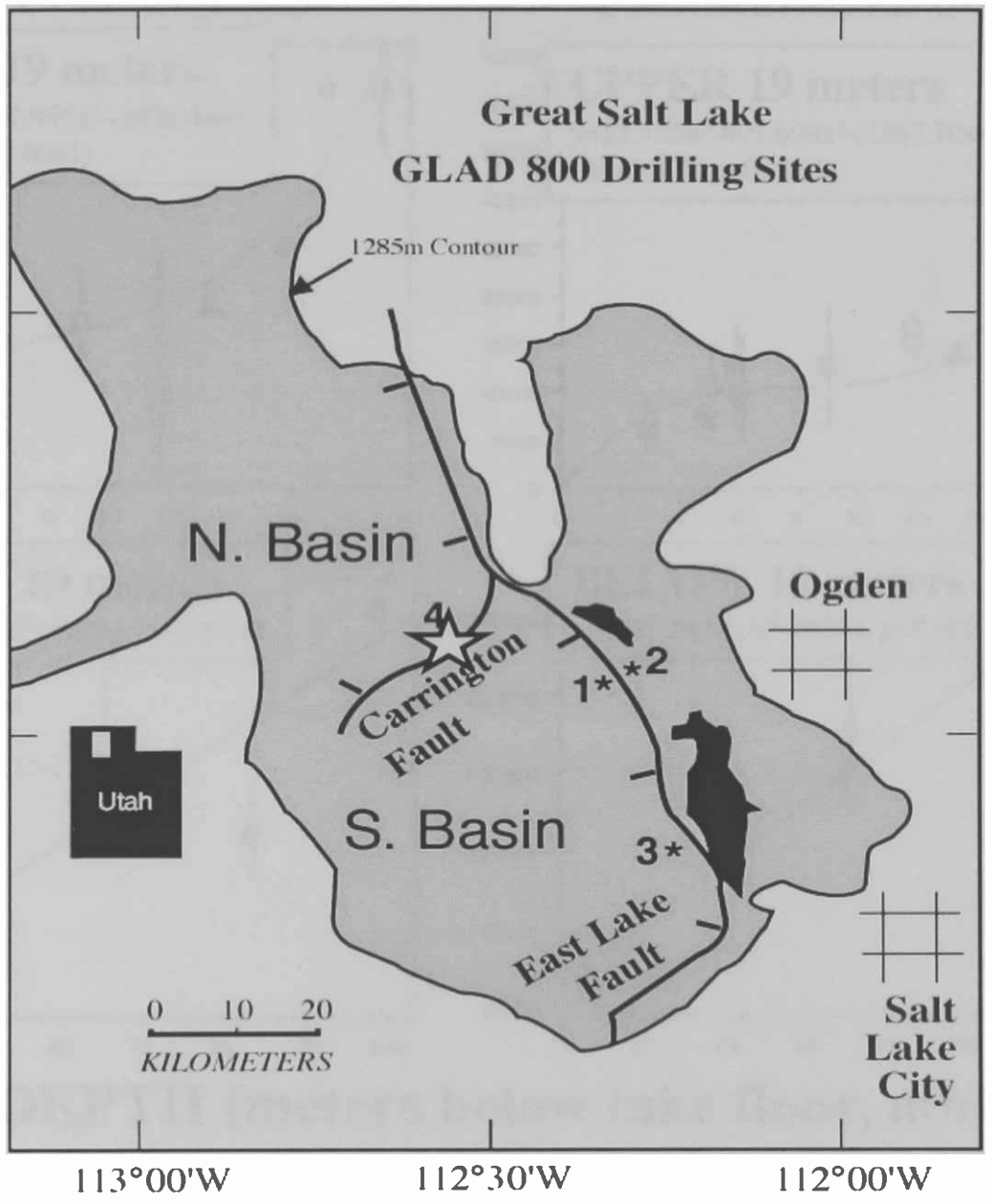
Great Salt Lake
GLAD 800 Drilling Sites
1285m Contour
N. Basin
Ogden
Carrington Fault
1*
*2
Utah
S. Basin
3*
East Lake Fault
0 10 20
KILOMETERS
Salt Lake City
41°30'N
41°00'N
113°00'W
112°30'W
112°00'W

Figure 1.

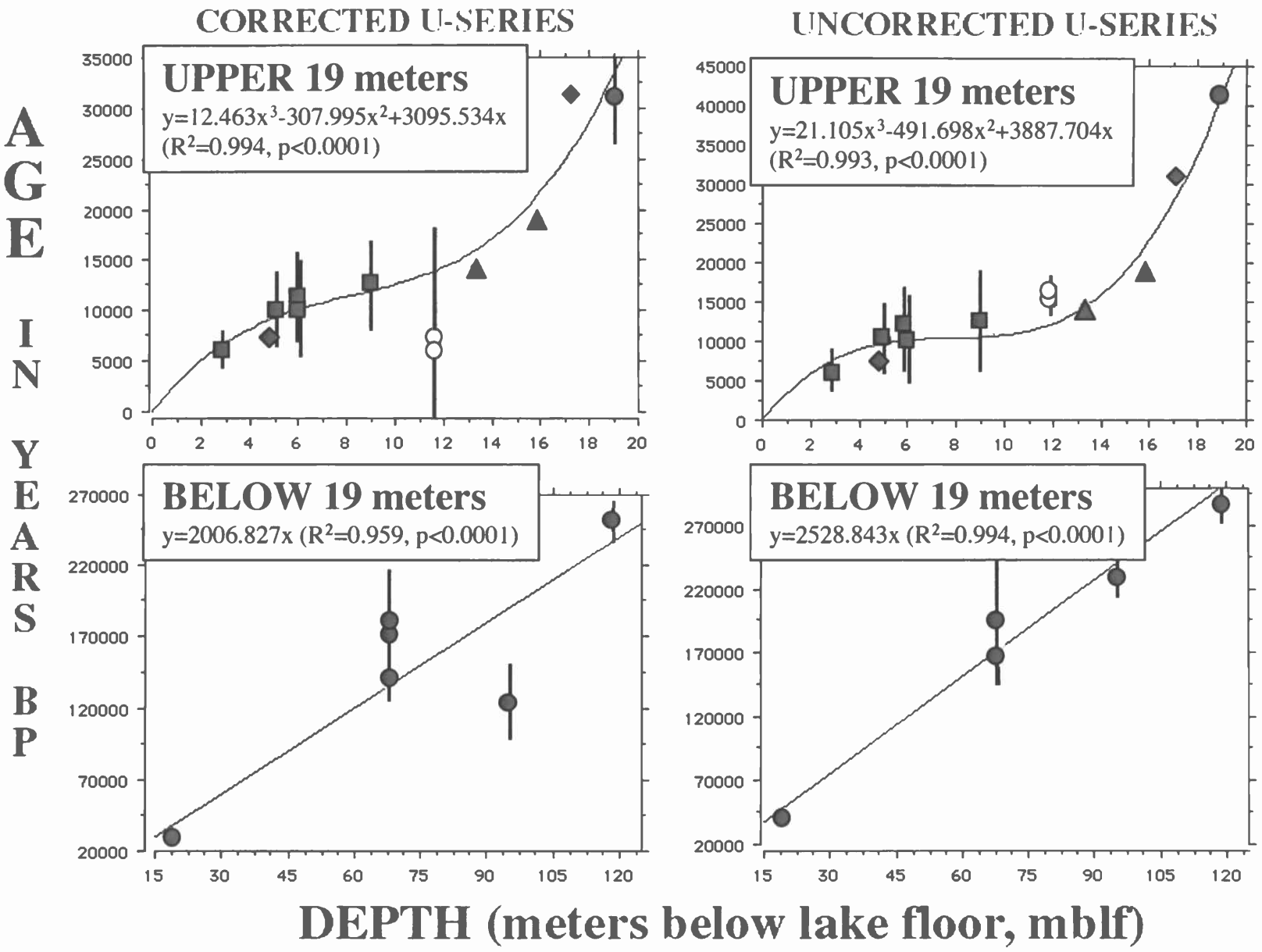
CORRECTED U-SERIES
UNCORRECTED U-SERIES
UPPER 19 meters
y=12.463x³-307.995x²+3095.534x
(R²=0.994, p<0.0001)
UPPER 19 meters
y=21.105x³-491.698x²+3887.704x
(R²=0.993, p<0.0001)
BELOW 19 meters
y=2006.827x (R²=0.959, p<0.0001)
BELOW 19 meters
y=2528.843x (R²=0.994, p<0.0001)
AGE IN YEARS BP
DEPTH (meters below lake floor, mblf)
Tephra
Biostratigraphic Correlation
Carbon-14
U-series (dates excluded from model○)

Figure 2.

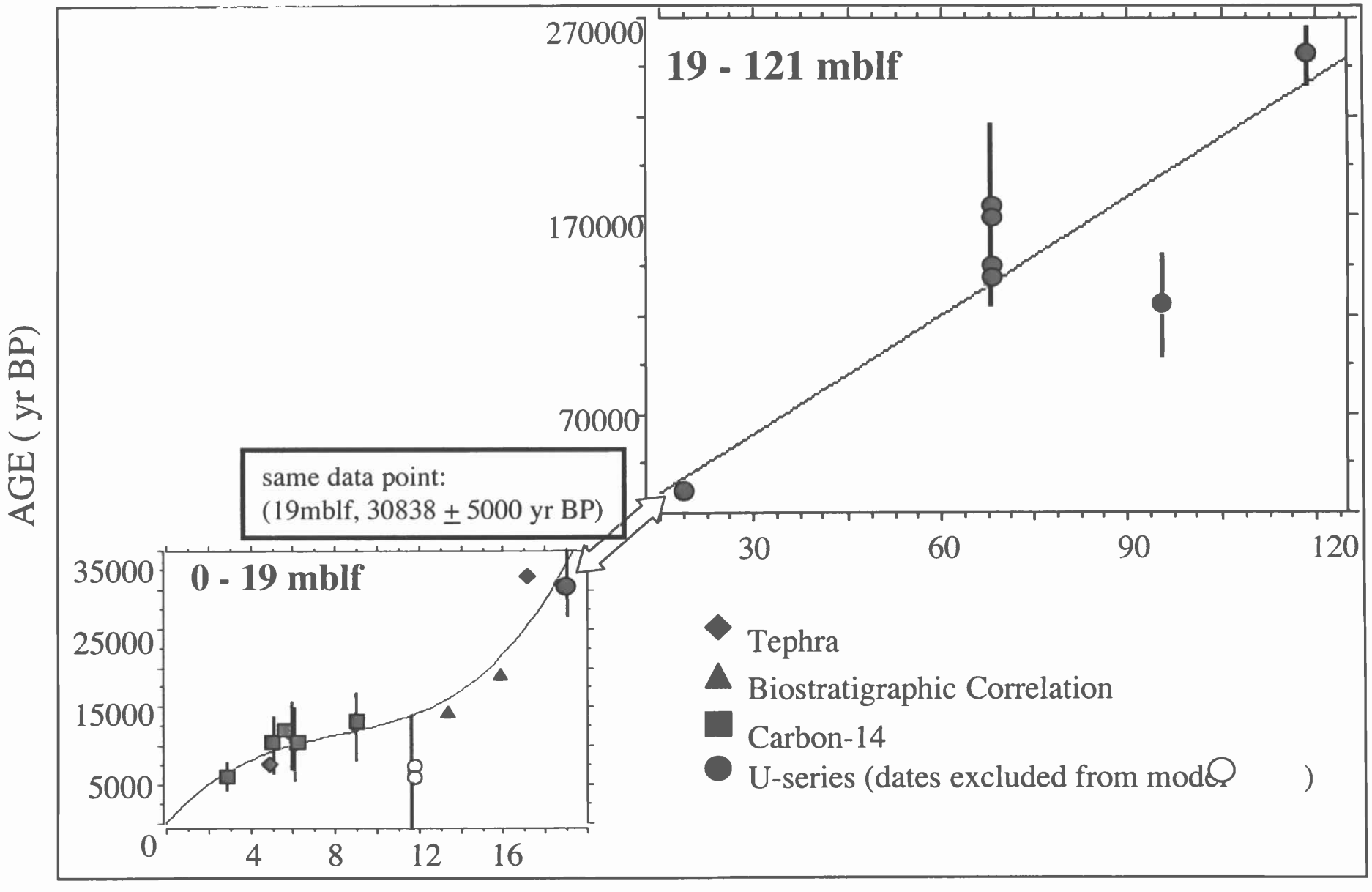
19 - 121 mblf
270000
170000
70000
30
60
90
120
same data point:
(19mblf, 30838 ± 5000 yr BP)
0 - 19 mblf
35000
25000
15000
5000
0
4
8
12
16
Tephra
Biostratigraphic Correlation
Carbon-14
U-series (dates excluded from mod
)
AGE (yr BP)
DEPTH (mblf)

Figure 3.

LITHOSTRATIGRAPY

- Gray carbonate clay/silt/mud
- Evaporite & muddy evaporites
- Laminated carbonate muds ± diatomaceous muds
- Carbonate muds ± mottled, roots, dewatering structures, soft sediment deformation
- Clay w/gypsum
- Massive-banded sands/silts muds (some mottling & bioturbation)

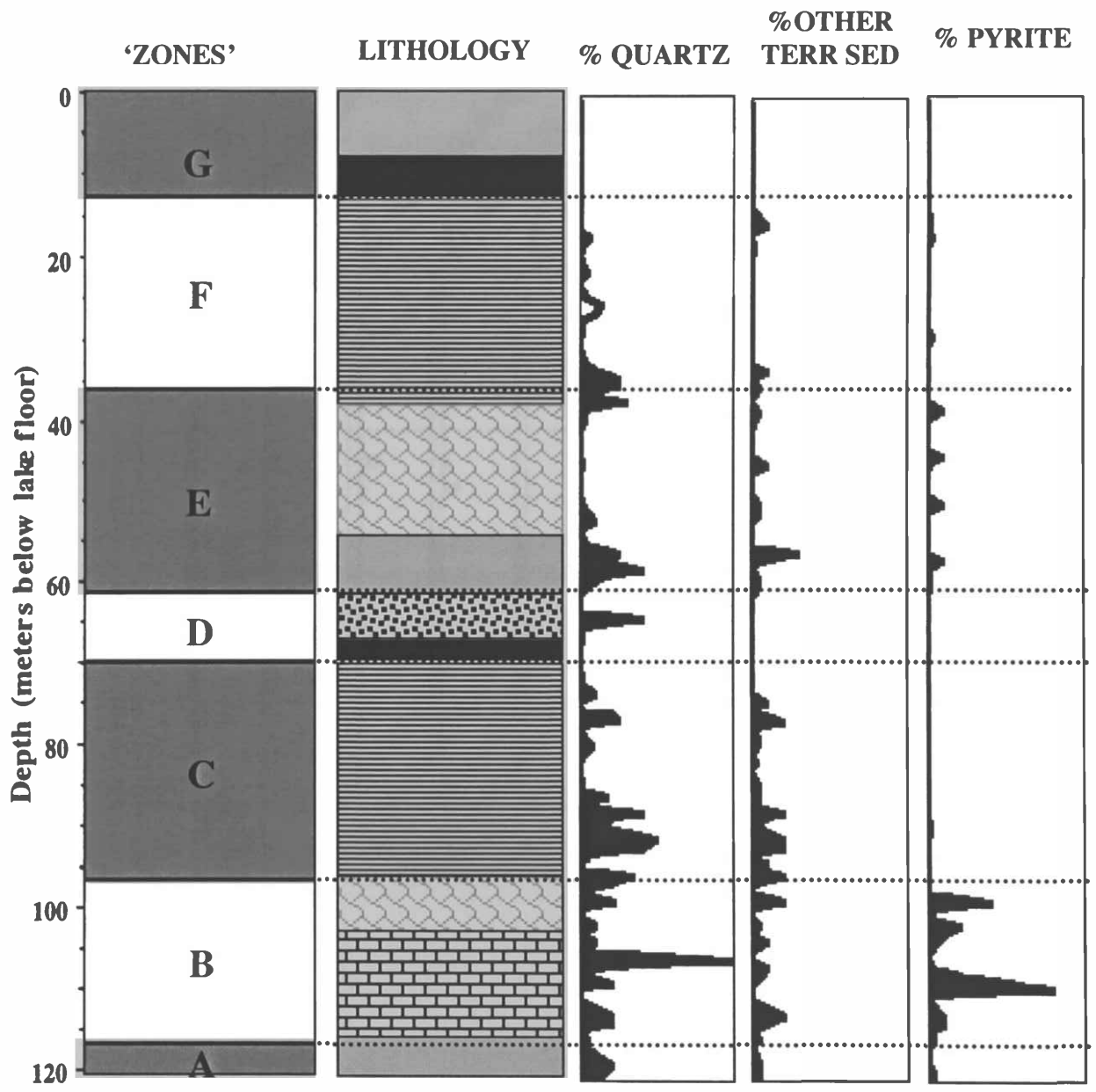

Figure 4.

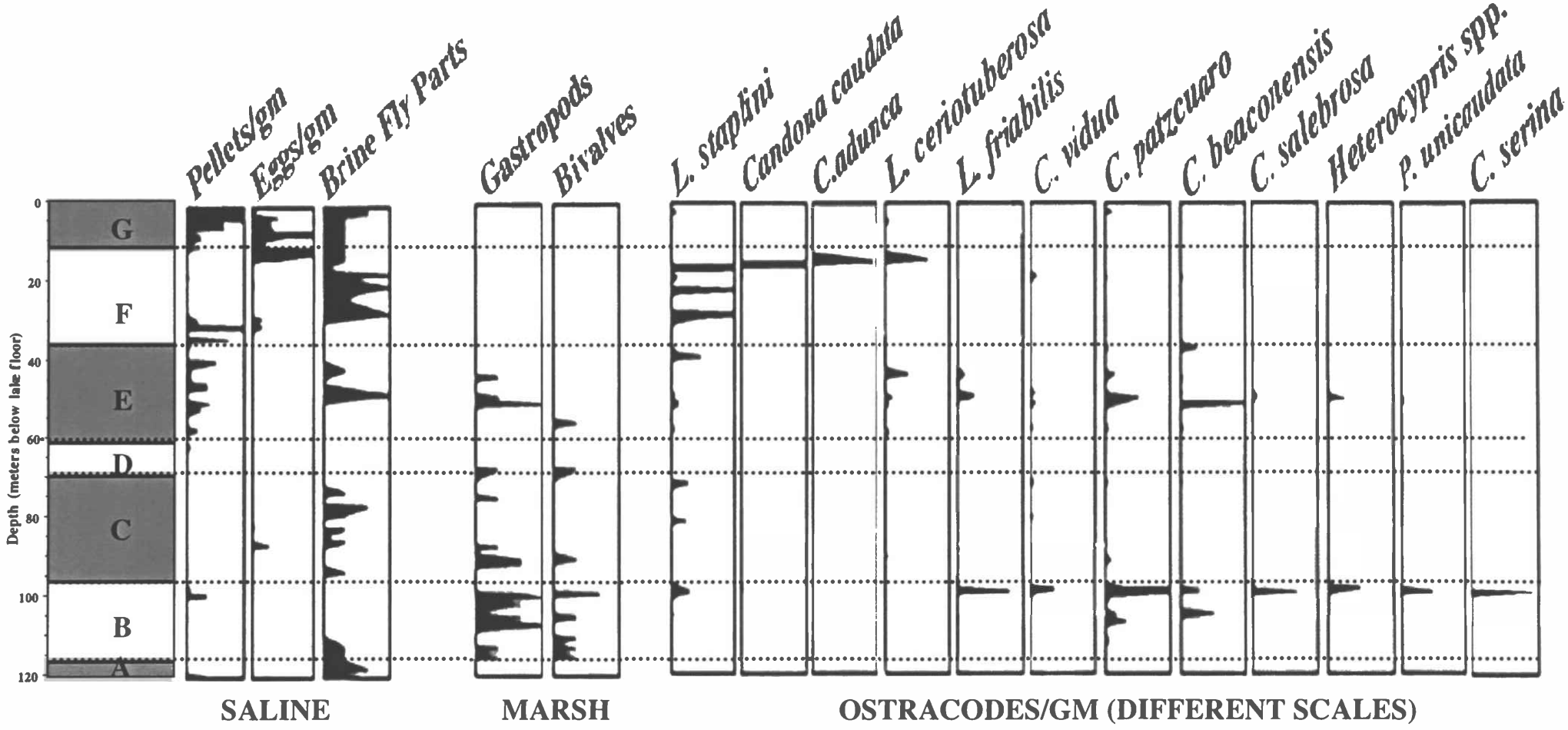
Pellets/gm
Eggs/gm
Brine Fly Parts
Gastropods
Bivalves
L. staplini
Candona caudata
C.aduncа
L. ceriotuberosa
L. friabilis
C. vidua
C. patzcuaro
C. beaconensis
C. salebrosa
Heterocypris spp.
P. unicaudata
C. serina
Depth (meters below lake floor)
0
20
40
60
80
100
120
G
F
E
D
C
B
A
SALINE
MARSH
OSTRACODES/GM (DIFFERENT SCALES)

Figure 5.

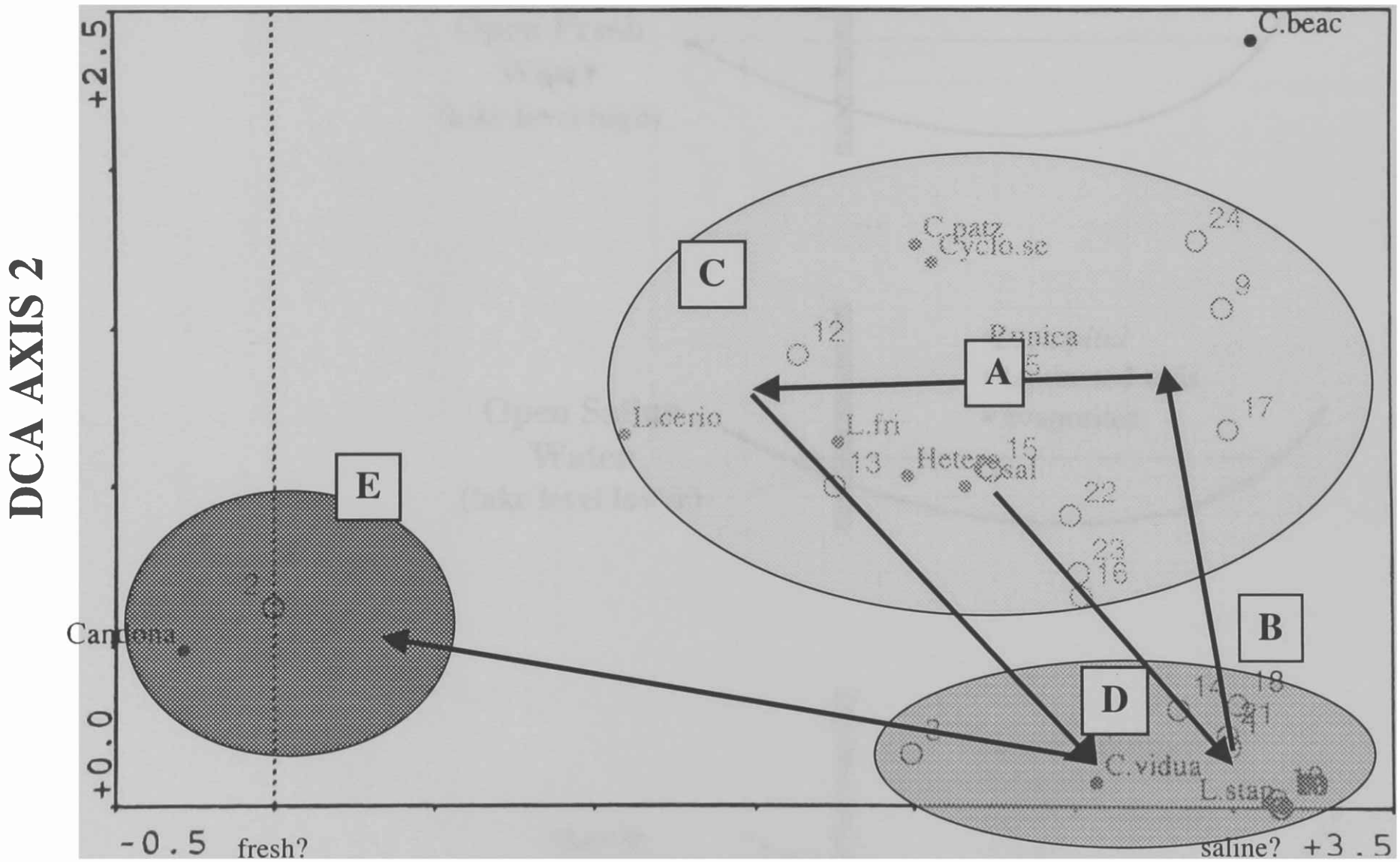
DCA AXIS 2
+2.5
+0.0
-0.5
fresh?
saline? +3.5
DCA AXIS 1
C.beac
C.patz
Cyclo.se
C
A
B
D
E
12
24
9
Panica
5
L.cerio
L.fri
13
Hetero
15
sal
22
23
16
17
14
18
21
Candona
C.vidua
L.stag

Figure 6.

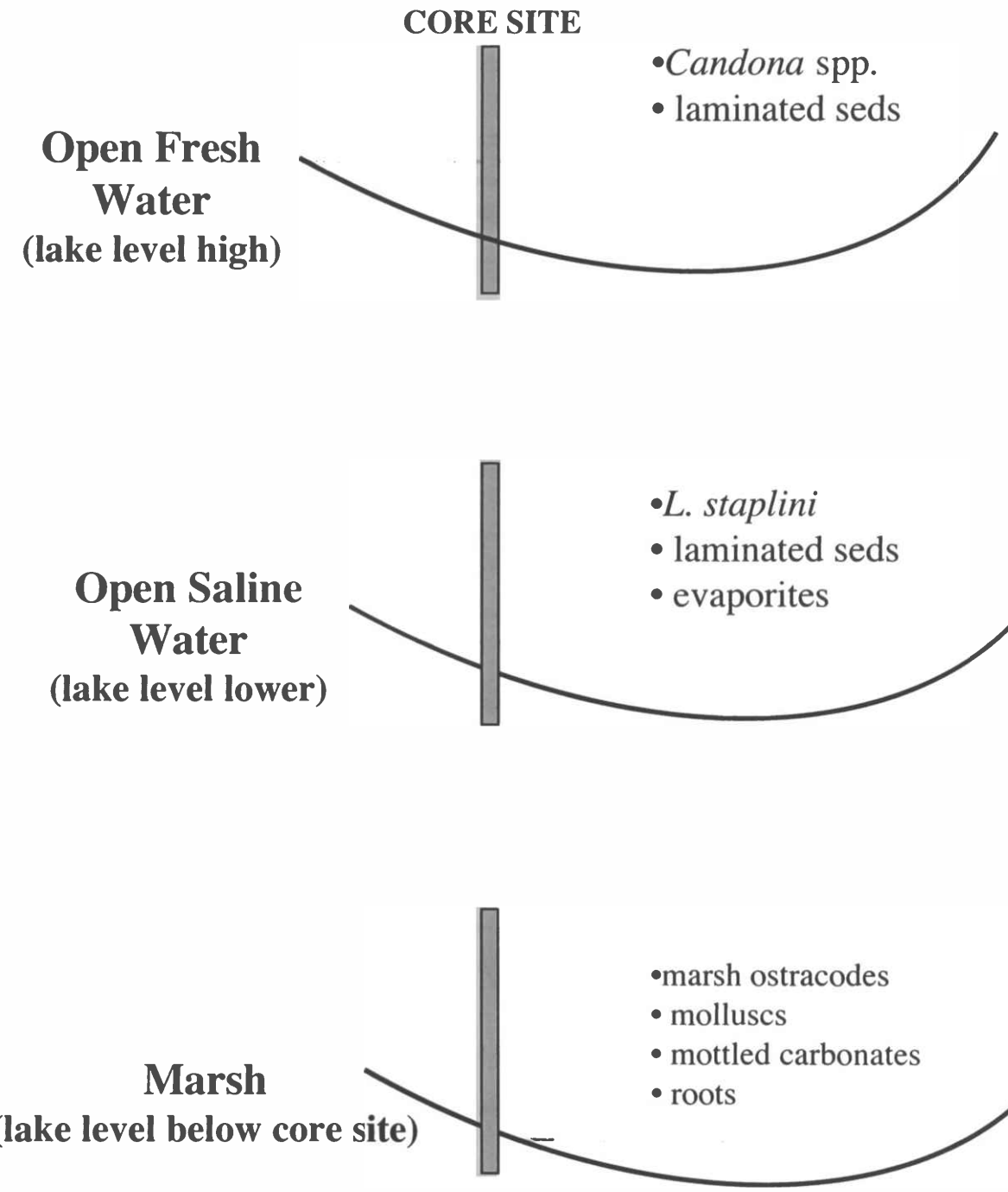
CORE SITE
Open Fresh Water
(lake level high)
•Candona spp.
• laminated seds
Open Saline Water
(lake level lower)
•L. staplini
• laminated seds
• evaporites
Marsh
(lake level below core site)
•marsh ostracodes
• molluscs
• mottled carbonates
• roots

Figure 7.

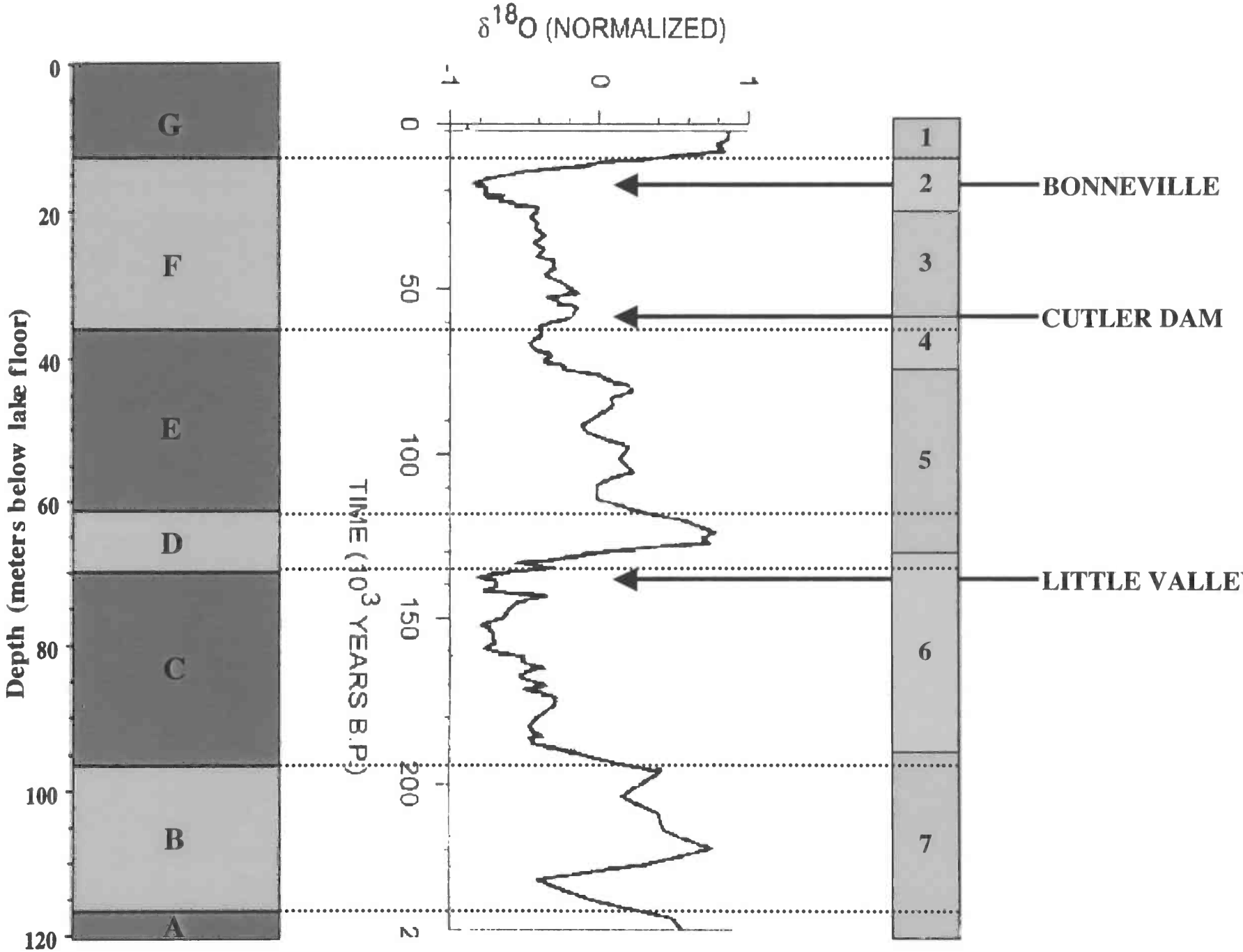
δ18O (NORMALIZED)
-1
0
1
0
50
100
150
200
TIME (10^3 YEARS B.P.)
Depth (meters below lake floor)
0
20
40
60
80
100
120
G
F
E
D
C
B
A
1
2
3
4
5
6
7
BONNEVILLE
CUTLER DAM
LITTLE VALLEY?
'ZONES'
SPECMAP (Martinson et al. 1987)
OIS

Figure 8.